

Most probable failure scenario in a model power grid with random power demand

Misha Stepanov and Aditya Sundararajan

Abstract—We consider a simple system with a local synchronous generator and a load whose power consumption is a random process. The most probable scenario of system failure (synchronization loss) is considered, and it is argued that its knowledge is virtually enough to estimate the probability of failure per unit time. We discuss two numerical methods to obtain the “optimal” evolution leading to failure.

Index Terms—failure probability, random power demand, rare events, optimal fluctuation.

I. INTRODUCTION

Whenever we use or design a system we are curious about its reliability. Failures may be very rare, still they could be of a tremendous importance, especially when the consequences are catastrophic and very undesirable. There is a huge amount of literature devoted to the study of power systems failures, for various situations and approaches see, *e.g.*, [1], [2], [3]. Failures could happen due to a hardware fault, because the realization of the system’s random component (noise) was an especially unlucky one (the latter is a focus of our work), or a combination of both.

While studying such unlucky realizations, one can ask the following questions: (1) What is the spatio-temporal shape/profile of the noise configuration that leads to a rare event/failure? (2) Is this shape universal? — If two unrelated failure events happen, will their pre-histories be alike?

Theoretical exploration of this subject started from the classical papers [4], [5], [6]. The theoretical approach is known under the names of optimal fluctuation or instanton method; it could also be viewed as a saddle-point method in functional space. It was originally introduced by I. M. Lifshitz [4] for analysis of electronic spectra of disordered systems, and was later developed to describe rare events in various fields, *e.g.*, quantum field theory [7], [8], statistical hydrodynamics [9], and power grids [10], [11].

The main conjecture of the optimal fluctuation method is a positive answer to the second question posed above. The rationale behind this theoretical expectation is as follows: In order to cause such a rare event, the deviation of the system’s random characteristics from their average values (*i.e.*, the noise) should be much larger than typical. On the other hand statistical weight, or probability, of the noise sharply

decays with the noise amplitude increase. On the whole variety of noise configurations leading to the event of interest the probability is highly peaked at the most probable or “optimal” configuration, on which the “amplitude” is not so very large, but the rare event still does happen due to carefully optimized shape of the noise.

Optimal fluctuation method consists in maximizing the probability of the random noise realization conditioned by the statement that the rare event of interest happens. In many cases one can come up with the [obviously problem specific] equations that the position of the maximum (*i.e.*, optimal fluctuation) should satisfy (with the meaning of the equations being “the derivative of the probability weight at the extremum is equal to zero”). These equations are often too complex for analytical solution and their numerical exploration remains the only feasible method of analysis.

The knowledge of optimal noise configuration can be indispensable for new system design, as it delivers important information on how dangerous and undesirable events are going to look like. Also, the probability [per unit time] of the rare event can be estimated.

In this work we consider a simple power system (Sec. II) and derive the equations the most probable failure scenario should satisfy (Sec. III, see also Sec. V). We present two numerical methods to solve these equations (Secs. IV and VI), and then discuss the probability of failure (Sec. VII).

II. EQUATIONS OF MOTION

Let us consider the following simple power system: It has 3 buses, one of them is a slack (or infinite) bus, another is a local synchronous generator bus, and the first two are connected by transmission lines to the 3rd one (a load bus), see Fig. 1. The dynamics of the system is governed by

$$\begin{aligned} M\dot{\phi} + D\dot{\phi} &= P_{\text{mech}} - \text{Re}(E_2 e^{i\phi} I_2^*), \\ iX_1 I_1 &= E_1 - V e^{i\phi/2}, \quad iX_2 I_2 = E_2 e^{i\phi} - V e^{i\phi/2}, \\ V e^{i\phi/2} (I_1 + I_2)^* &= S(t) = P(t) + iQ(t), \end{aligned} \quad (1)$$

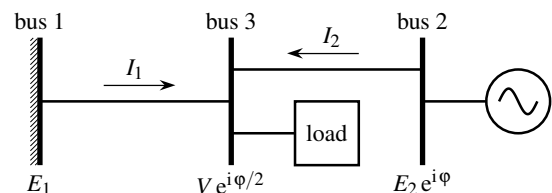


Fig. 1. Model power system. The currents I_1 and I_2 , and the voltage V are complex numbers.

This work was supported by DTRA/DOD grant BRCALL06-Per3-D-2-0022 “Network adaptability from WMD disruption and cascading failures”.

M. Stepanov is with Department of Mathematics, University of Arizona, Tucson, AZ 85721, USA (e-mail: stepanov@math.arizona.edu).

A. Sundararajan is with Department of Electrical and Computer Engineering, University of Arizona, Tucson, AZ 85721, USA (e-mail: adityas@email.arizona.edu).

where X_1 and X_2 are reactances of the lines, P_{mech} is an input of mechanical power which we assume constant, and P/Q is the real/reactive power consumed by the load. The eq. (1) is the swing equation with M being the moment of inertia of the generator divided by a square of the number of “poles” (*i.e.*, how many oscillations of voltage one rotation of the generator produces) and multiplied by angular frequency of rotation. The term $D\dot{\varphi}$ describes damping in the generator. The dot over a variable denotes a time derivative, two dots mean second time derivative. The asterisk $*$ represents the complex conjugate. By excluding I_1 and I_2 we get

$$\begin{aligned} M\ddot{\varphi} + D\dot{\varphi} &= P_{\text{mech}} - (E_2/X_2) \text{Im}(V^* e^{i\varphi/2}), \\ S &= iV \left(\frac{E_1 e^{i\varphi/2}}{X_1} + \frac{E_2 e^{-i\varphi/2}}{X_2} \right) - i|V|^2 \left(\frac{1}{X_1} + \frac{1}{X_2} \right). \end{aligned}$$

Let us consider $X_1 = X_2 = 1$, $E_1 = E_2 = 1$, $M = 1$. We will also write $V = y - ix$. We have

$$\begin{aligned} \ddot{\varphi} + D\dot{\varphi} &= P_{\text{mech}} - Cx - Sy, \\ P &= 2Cx, \quad Q = 2Cy - 2(x^2 + y^2). \end{aligned}$$

where $C = \cos(\varphi/2)$, $S = \sin(\varphi/2)$. The boundary for the solution existence for x and y is given by the inequality $Q \leq (C^2 - P^2/C^2)/2$. We will assume $Q = kP$ with some constant k (constant power load model [12], although we will allow the power demand P to change in time). We will use the value $k = 3/4$, and the inequality becomes $P \leq C^2/2$.

Let us consider as a Normal Operating Point (NOP) the steady-state (*i.e.*, $\dot{\varphi} = \ddot{\varphi} = 0$) solution with

$$\begin{aligned} \varphi_* &= 0, \quad C_* = 1, \quad S_* = 0, \\ S_* &= P_* + iQ_* = (4 + 3i)/16, \quad P_{\text{mech}} = 1/8, \\ V_* &= y_* - ix_* = (7 - i)/8. \end{aligned}$$

The dynamics of the system depends on many concrete implementation details, *e.g.*, how the situations when the power flow problem has several solutions or does not have a solution satisfying all load demands are resolved. The dynamics may be altered by the presence of various control devices. We will use the equation

$$\begin{aligned} \ddot{\varphi} + D\dot{\varphi} &= P_{\text{mech}} - \mathcal{P}(P, \varphi), \\ \mathcal{P}(P, \varphi) &= \underbrace{\frac{P_{\text{supp}}}{2}}_{C_x} + \underbrace{\frac{S}{2} \left(C + \sqrt{C^2 - \frac{3P_{\text{supp}}}{2} - \frac{P_{\text{supp}}^2}{C^2}} \right)}_{S_y}, \end{aligned} \quad (2)$$

where $P_{\text{supp}} = \min(P, C^2/2)$ — the power demand greater than $C^2/2$ cannot be fulfilled. The “+” sign at the square root in the expression for \mathcal{P} is, let us say, a reflection of some kind of voltage control, where higher voltage (larger y) is chosen from the two possible solutions.

The phase portrait of the system for the case of power demand $P(t) \equiv P_* = 1/4$ is shown in Fig. 2. The NOP $\varphi = \dot{\varphi} = 0$ is a stable focus. When $|\varphi| > \pi/2$ we have $P_{\text{supp}} = C^2/2$ and $V = y - ix = C(2 - i)/4$. The voltage at the load is small when φ is close to π or $-\pi$.

The system is stable to sudden but permanent changes of the power demand: *E.g.*, if P is suddenly dropped to 0, then the dynamics just goes to the new fixed point, see Fig. 3.

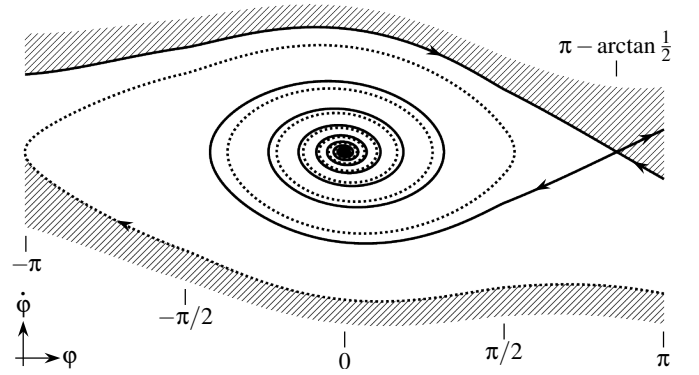


Fig. 2. Phase portrait of the system (2) with $P(t) \equiv P_* = 1/4$. Here and in all other $(\varphi, \dot{\varphi})$ -plots the scales of φ and $\dot{\varphi}$ are the same and $D = 0.1$. Shading shows the regions where the dynamics eventually leads to $\varphi = \pi$ or $\varphi = -\pi$.

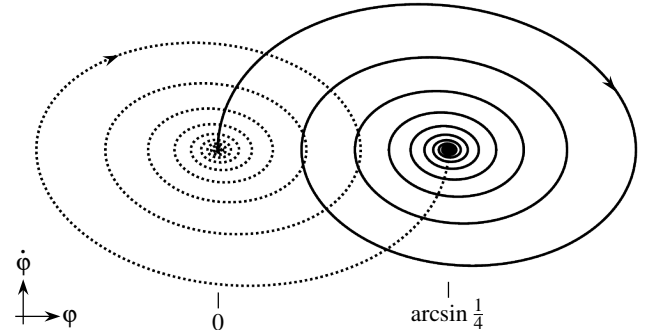


Fig. 3. Response of the system to a sudden change of consumed power: trajectories with $P = 0$ starting from $\varphi = \dot{\varphi} = 0$ (solid curve) and with $P = P_* = 1/4$ starting from $\varphi = \arcsin \frac{1}{4}$, $\dot{\varphi} = 0$ (dotted curve).

III. OPTIMAL FLUCTUATION EQUATIONS

Consider the case when the power demand $P(t)$ is a random process or can be changed in time in a controlled way. How the power system can be brought out of the stable equilibrium $\varphi = \dot{\varphi} = 0$, $P = P_*$ to a voltage collapse $\varphi = \pm\pi$? (Even smaller angles φ could be viewed as an unacceptable loss of synchronization. In this work, as an example, will consider the model system “failure” being $\varphi = \pm\pi$.)

Somewhat barbaric but reliable way is to choose $P(t)$ with minimal/maximal value of $\mathcal{P}(P, \varphi)$ when $\dot{\varphi} > 0/\dot{\varphi} < 0$. How in this case the power demand P should be chosen is shown in Fig. 4. Besides the case of $\dot{\varphi} < 0$, $0 < \varphi < 2\arccos \frac{3}{5} = 4\arctan \frac{1}{2}$, the demand P is equal to extreme supported values: $P = 0$ or $P = C^2/2$. The resulting trajectories leading to $\varphi = \pi$ are shown as thick curves in Fig. 5.

The Most Probable Failure Scenario (MPFS) depends on the statistics of the random process $P(t)$. (When using optimal fluctuation method for practical applications this should be kept in mind, and as much properties of the system’s random component should be extracted experimentally as seems feasible.¹) In this work, as an example, we will use probably the most simple yet not entirely unrealistic probabilistic model

¹The statistics of the state of a power grid at a given time can be written through a functional integral [13]. This is especially useful when a random noise in the system is correlated in time. When finding the [small] probability of failure, the integral often can be estimated by the method of steepest descent, with MPFS trajectory being the saddle point.

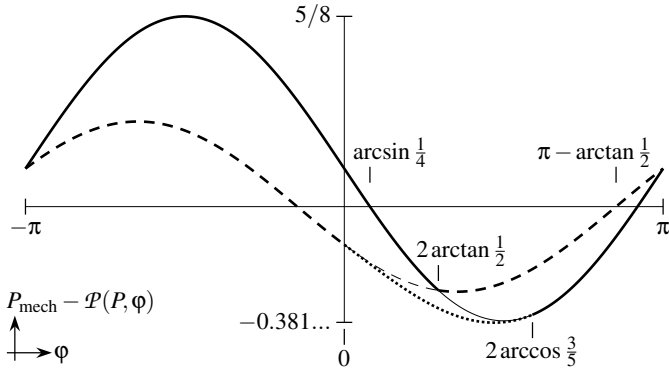


Fig. 4. Extreme possible values of $P_{\text{mech}} - \mathcal{P}(P, \varphi)$, that are realized at $P = 0$ (solid curve), $P \geq C^2/2$ (dashed curve), and $P = C^2(5C - 3)/4$ (dotted curve).

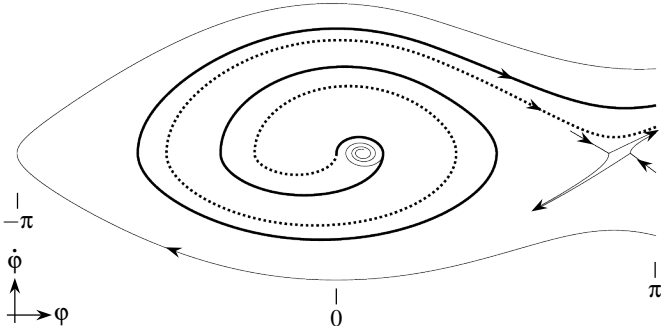


Fig. 5. Phase portrait of the system (2) with P at each moment of time being chosen in order to have maximal if $\dot{\varphi} > 0$ and minimal if $\dot{\varphi} < 0$ possible value of thrust $P_{\text{mech}} - \mathcal{P}(P, \varphi)$ (see Fig. 4). Thick solid/dotted curve corresponds to starting condition being NOP $\varphi = 0$, $\dot{\varphi} = 0$, with the initial thrust in positive/negative direction. Thin spiral near the center is the [solid curve] trajectory from Fig. 3 shown here for comparison.

for $P(t)$: There are Λ customers, and during each small chunk of time δ each customer either consumes electricity or not, independently of other customers and other moments of time. For each chunk of time the power demand is binomially distributed. We will assume that $\Lambda \gg \lambda \gg 1$, where λ is the average number of customers consuming electricity at a given time. The binomial distribution is then approximated by Poisson: $P(n) = \lambda^n e^{-\lambda}/n! \approx \lambda^n \exp(-\lambda H(n/\lambda))/\sqrt{2\pi n}$ with convex Cramér function $H(x) = 1 - x + x \ln x$.

If we track the evolution of the system over time interval T , then there are T/δ chunks of time. The probability that there are n_k active customers in k^{th} chunk of time is

$$\prod_{k=1}^{T/\delta} P(n_k) \approx \exp\left(-\lambda \sum_{k=1}^{T/\delta} H(n_k/\lambda)\right) / \prod_{k=1}^{T/\delta} \sqrt{2\pi n_k}. \quad (3)$$

When δ is small, the sum over k in the exponent could be approximated by an integral over time.

The problem of finding out which failure development is the most probable boils down to the following problem of optimal control: Find the power consumption $P(t)$, $t_0 \leq t \leq t_1$ such that $\varphi(t_0) = \omega(t_0) = 0$ (NOP) and $|\varphi(t_1)| = \pi$ (failure), and the integral $\mathcal{S} = \int_{t_0}^{t_1} dt H(P(t)/P_*)$ has the minimal possible value. We can fix the time of failure t_1 to 0. As we do not care how

²Stirling's approximation: if n is large, then $n! \approx \sqrt{2\pi n} (n/e)^n$.

fast the transition from NOP to the failure happens, we have to consider $t_0 = -\infty$.

Consider an equation of motion $\dot{\mathbf{x}} = \mathbf{f}(\mathbf{x}, \mathbf{u})$. We want to move from $\mathbf{x}_{\text{start}}$ to \mathbf{x}_{end} in such a way that the integral over time of $H(\mathbf{u})$ is minimal. Let us construct the functional

$$\begin{aligned} \mathcal{S}\{\underbrace{\mathbf{x}, \mathbf{u}, \alpha, \boldsymbol{\beta}}_{\text{functions of } \tau}, \boldsymbol{\gamma}_{0,1}\} &= \boldsymbol{\gamma}_0(\mathbf{x}(\tau_0) - \mathbf{x}_{\text{start}}) + \boldsymbol{\gamma}_1(\mathbf{x}(\tau_1) - \mathbf{x}_{\text{end}}) \\ &+ \int_{\tau_0}^{\tau_1} d\tau \boldsymbol{\beta}(\tau) \left(\frac{d\mathbf{x}}{d\tau} - \alpha \mathbf{f}(\mathbf{x}, \mathbf{u}) \right) + \int_{\tau_0}^{\tau_1} d\tau \alpha(\tau) H(\mathbf{u}(\tau)), \end{aligned}$$

where $\boldsymbol{\beta}(\tau)$, $\boldsymbol{\gamma}_{0,1}$ are Lagrange multipliers enforcing the equation for \mathbf{x} and boundary conditions, respectively. The function $\alpha(\tau)$ is introduced to arbitrarily parametrize the time t ($dt = \alpha d\tau$), this trick³ allows us to have fixed limits of integration $\tau_{0,1}$ (we can choose any values, e.g., $\tau_0 = 0$ and $\tau_1 = 1$).

Setting the variation over various variables in in \mathcal{S} to zero we get Euler–Lagrange equations

$$\boldsymbol{\beta} : \dot{\mathbf{x}} = \mathbf{f}(\mathbf{x}, \mathbf{u}), \quad (4)$$

$$\mathbf{x} : \dot{\boldsymbol{\beta}}_i = -\boldsymbol{\beta} \cdot \partial \mathbf{f} / \partial x_i, \quad (5)$$

$$\alpha : H(\mathbf{u}) - \boldsymbol{\beta} \cdot \mathbf{f}(\mathbf{x}, \mathbf{u}) = 0, \quad (6)$$

$$\mathbf{u} : \mathbf{u} \text{ minimizes } H(\mathbf{u}) - \boldsymbol{\beta} \cdot \mathbf{f}(\mathbf{x}, \mathbf{u}). \quad (7)$$

From the structure of the expression for \mathcal{S} another view on α is that it is a Lagrange multiplier enforcing eq. (6).

If one considers the dynamics in $(\mathbf{x}, \boldsymbol{\beta}, \mathbf{u})$ space (of dimension $2D_x + D_u$, where $D_x = D_{\boldsymbol{\beta}}$ and D_u are the lengths of vectors \mathbf{x} and \mathbf{u} ; in our model system $D_x = 2$ and $D_u = 1$), then the eqs. (6) and (7) produce a $(2D_x - 1)$ -dimensional surface in it. The equations of motion (4) and (5) determine the direction of movement, which gives another $(2D_x - 1)$ conditions. From naive dimensions counting one could think that together all the equations are satisfied at isolated points. This is not true.

In a “good” case, when all functions are differentiable, because of the eqs. (4), (5), and (7) the quantity $\mathcal{H} = H(\mathbf{u}) - \boldsymbol{\beta} \cdot \mathbf{f}(\mathbf{x}, \mathbf{u})$ is conserved, $d\mathcal{H}/dt = 0$, so the eq. (6) is automatically kept true, and all the equations are satisfied along 1-dimensional [optimal] trajectories. The eq. (7) is Pontryagin’s minimum principle with \mathcal{H} being the Hamiltonian⁴, the eq. (5) is the costate equation, and the eq. (6) reflects that the evolution time is not fixed [14].

For our model power grid we have

$$\frac{d}{dt} \underbrace{\begin{bmatrix} \varphi \\ \omega \end{bmatrix}}_{\mathbf{x}} = \underbrace{\begin{bmatrix} \omega \\ -D\omega + P_{\text{mech}} - \mathcal{P}(P, \varphi) \end{bmatrix}}_{\mathbf{f}(\mathbf{x}, \mathbf{u})}, \quad (4a)$$

$$\frac{d}{dt} \underbrace{\begin{bmatrix} \beta_\varphi \\ \beta_\omega \end{bmatrix}}_{\boldsymbol{\beta}} = \underbrace{\begin{bmatrix} \beta_\omega \partial \mathcal{P}(P, \varphi) / \partial \varphi \\ D\beta_\omega - \beta_\varphi \end{bmatrix}}, \quad (5a)$$

$$\beta_\varphi = \frac{1}{\omega} \left(H(P/P_*) + \beta_\omega (D\omega - P_{\text{mech}} + \mathcal{P}(P, \varphi)) \right). \quad (6a)$$

³We could introduce \mathcal{S} with integral over time t from 0 to T (or make $\alpha \equiv 1$, $\tau = t$, and $\tau_0 = 0$, $\tau_1 = T$), and then try to find the minimum in T . This may be technically cumbersome as it would involve derivatives of $\mathbf{x}(t)$ and $\mathbf{u}(t)$ with respect to T .

⁴We have $\dot{x}_i = -\partial \mathcal{H} / \partial \beta_i$ and $\dot{\beta}_i = \partial \mathcal{H} / \partial x_i$.

Let us discuss two issues with these equations. *First*, sometimes the eq. (7) prescribes $P = C^2/2$, and then the derivative $\partial \mathcal{P}(P, \varphi)/\partial \varphi$ does not exist (or is infinite). In this case β_φ could rapidly change in time, and its value should be chosen so that the eq. (6a) is maintained.

Second, if $\omega = 0$, then how the eq. (6a) should be understood? When $\omega = 0$ the movement in the $(\varphi, \dot{\varphi})$ phase plane is directed vertically no matter what is the value of P . As the time of the evolution is not important for us, we don't care how fast we are moving if the direction of movement is the same. Thus, in order to minimize $\int dt H(P/P_*)$ we have to choose $P = P_*$. On the MPFS trajectory we have $P(t) = P_*(1 + \omega(t)\rho(t))$ with ρ being finite at $\omega = 0$. To get that from the eq. (7) we need to have $\beta_\omega = \omega\beta$ with finite β . The eq. (6a) is then non-singular⁵ at $\omega = 0$. The MPFS equations become

$$\dot{\varphi} = \omega, \quad \dot{\omega} = -D\omega + P_{\text{mech}} - \mathcal{P}(P_*(1 + \omega\rho), \varphi), \quad (4b)$$

$$\dot{\beta} = D\beta - H(1 + \omega\rho)/\omega^2, \quad (5,6b)$$

$$\rho \text{ minimizes } H(1 + \omega\rho) + \omega\beta\mathcal{P}(P_*(1 + \omega\rho), \varphi). \quad (7b)$$

When β is small, then due to the eq. (7b) ρ is small too, and in the eq. (5,6b) the value of β never changes sign. In MPFS β is positive. Positive/negative $\omega\beta$ (or just ω) bias the thrust $P_{\text{mech}} - \mathcal{P}(P, \varphi)$ to larger/smaller values, and that causes NOP to be unstable. When $|\omega\beta| \gg 1$ the extreme values of thrust, as in Fig. 4, are realized.

IV. NUMERICAL SOLUTION FROM IVP

The MPFS equations (4b–7b) form a non-linear Boundary Value Problem (BVP). Here we show how it can be treated as an Initial Value Problem (IVP). (This can be viewed as a kind of analog of the shooting (from $t = -\infty$) method.) Let us consider the linearization of MPFS equations near the NOP solution $\varphi = \omega = 0$:

$$\dot{\varphi} = \omega, \quad \dot{\omega} = -D\omega - \omega\rho/8 - 7\varphi/16, \quad (4c)$$

$$\dot{\beta} = D\beta - \rho^2/2, \quad \rho = -\beta/8. \quad (5,6,7c)$$

There are two steady state solutions: $\beta = \rho = 0$, *i.e.*, $P = P_*$ (stable in φ and ω , unstable in β direction, this solution is not interesting for us⁶); and $\beta = 128D$, $\rho = -16D$ which will give us the MPFS trajectory.

We solve (until failure) the IVP eqs. (4b–7b) with the initial data $\varphi_{\text{start}} = 0$, $\omega_{\text{start}} = \varepsilon \ll 1$, and $\beta_{\text{start}} = 128D$. Initially, while $\rho \approx -16D$, the eqs. (4c) look like $\dot{\varphi} = \omega$, $\dot{\omega} = D\omega - 7\varphi/16$, and NOP $\varphi = \omega = 0$ is an unstable focus — the IVP solution is periodic in $\log \varepsilon$ (this can be interpreted as going from one swirl to the next one in the spiral). We need to cover just one period to get all solutions. From this 1-dimensional family of solutions we need to pick the one with the minimal value of $\int dt H(P(t)/P_*)$.

The resulted MPFS trajectory is shown in Figs. 6 and 7, see also Fig. 8. In Fig. 9 one can see the buildup of $\mathcal{S} =$

⁵The change of variables $P, \beta_\omega \rightarrow \rho, \beta$ made by division by ω is an example of singularity resolution by “blowing up”.

⁶The equations (4–7) for $\dot{\mathbf{x}} = \mathbf{f}(\mathbf{x}, \mathbf{u})$ support solution $\beta \equiv \mathbf{0}$, \mathbf{u}_* minimizes $H(\mathbf{u})$ with $H(\mathbf{u}_*) = 0$. It works if we reach \mathbf{x}_{end} from $\mathbf{x}_{\text{start}}$ in a relaxed manner, *i.e.*, with $\mathbf{u} \equiv \mathbf{u}_*$.

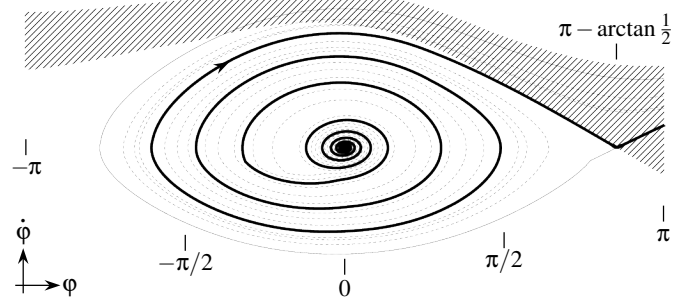


Fig. 6. MPFS trajectory constructed with $\varepsilon = \varepsilon_0 \approx 1.03452 \cdot 10^{-12}$. Three dashed thin line trajectories are built with $\varepsilon = \varepsilon_0 F^{1/4}$, $\varepsilon_0 F^{1/2}$, and $\varepsilon_0 F^{3/4}$, where $F = \exp(2\pi D/\sqrt{7/4 - D^2})$ (trajectory with $\varepsilon = \varepsilon_0 F$ would almost coincide with the one with $\varepsilon = \varepsilon_0$). The thin line trajectory coming from the saddle at $\varphi = \pi - \arctan \frac{1}{2}$ uses ε that is slightly less than ε_0 .

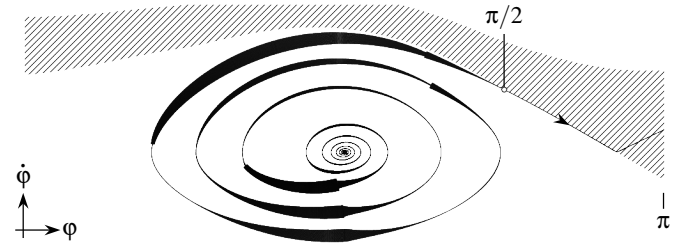


Fig. 7. MPFS trajectory constructed with $\varepsilon = \varepsilon_0 \approx 1.03452 \cdot 10^{-12}$. The thickness of the line is equal to $(H(P/P_*) + 0.01) \cdot 12$ pt. The trajectory point at $\varphi = \pi/2$ is right on the border of the shaded region.

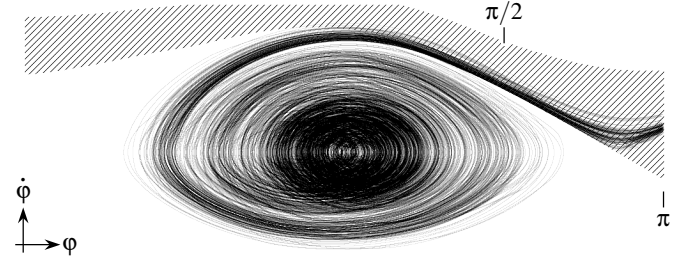


Fig. 8. 100 failure trajectories obtained by direct numerical simulation of (2) with $\lambda = 2$ and $\delta = 1.5$ (mean time to failure is about $4.8 \cdot 10^7$). On each trajectory the last 100 time units before reaching $\varphi = \pi$ are shown.

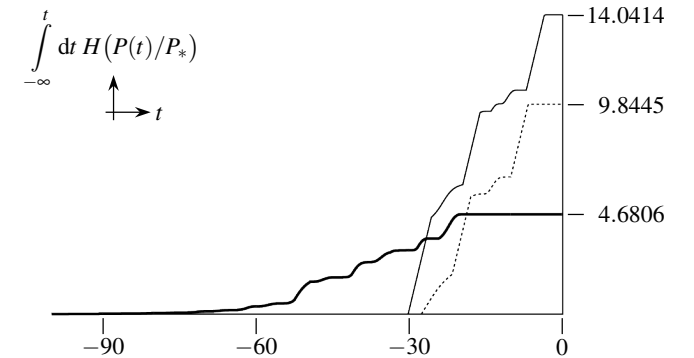


Fig. 9. The growth of cost function $\mathcal{S}(t) = \int_{-\infty}^t dt H(P(t)/P_*)$ in time. The value of $\mathcal{S} = \mathcal{S}(0)$ is indicated by numbers on the right. Thin solid and dashed curves correspond to “barbaric” trajectories from Fig. 5. The plateau on the thick curve near $t = 0$ is technically infinitely wide, as MPFS trajectory passes through the saddle at $\varphi = \pi - \arctan \frac{1}{2}$, $\dot{\varphi} = 0$.

$\int_{-\infty}^0 dt H(P/P_*)$ in time and comparison of \mathcal{S} values on the optimal trajectory and the ones from Fig. 5.

Obtaining the solution from IVP is not going to work well for large systems. When the dimension D_x of vector \mathbf{x} is large, it is hard to pick the most probable trajectory from $(D_x - 1)$ -dimensional family of IVP solutions.

V. HAMILTON–JACOBI–BELLMAN EQUATION

Let us introduce the following value function: $\mathcal{S}(\varphi, \dot{\varphi}; T)$ is the minimal value of integral of $H(P(t)/P_*)$ over time on the trajectory that starts at $(\varphi, \dot{\varphi})$ and reaches $\varphi = \pm\pi$ during the time *less or equal* to T . (If such a trajectory does not exist, then let us define $\mathcal{S} = +\infty$.) This function satisfies the Hamilton–Jacobi–Bellman (HJB) equation.

We are interested in $\mathcal{S}(\varphi, \dot{\varphi}) = \lim_{T \rightarrow \infty} \mathcal{S}(\varphi, \dot{\varphi}; T)$ (we care about the overall probability of the failure, not in how much time is needed for it to develop); and more specifically in $\mathcal{S}(0, 0)$, which corresponds to NOP as the starting state. The *time-independent* HJB equation in this case are the eqs. (6) and (7), with $-\boldsymbol{\beta}$ being the gradient of the value function $\mathcal{S}(\varphi, \dot{\varphi})$. The eq. (6) determines the rate of change of $\int dt H(P/P_*)$ through this gradient and the equation of motion.

From Fig. 4 we see that when $\varphi > 2\arctan \frac{1}{2}$ the most effective way to push the system to the right is to choose $P \geq C^2/2$. If $\varphi > \pi/2$, then $C^2/2 < P_*$, so $P = P_*$ is both the most effective and the most probable. If the system didn't reach the upper shaded region in Fig. 2 before $\varphi = \pi/2$, then it will not be able to reach the saddle at $\varphi = \pi - \arctan \frac{1}{2}$ and will be pushed back to the left. The optimal trajectory should pass through the border point of the shaded region at $\varphi = \pi/2$, see also Fig. 7.

The function $\mathcal{S}(\varphi, \dot{\varphi})$ is not continuous and undergoes a jump along the $\pi/2 < \varphi < \pi$ part of the border of the shaded region. The height of the jump is the integral of $H(P/P_*)$ along the additional [penalty] loop. In power grids with bounds on the possible dynamics due to, *e.g.*, existence of power flow solution regions or maximum allowed currents through lines, such discontinuities should be a commonplace.

In general situation a time-independent value function can be introduced if the random process describing fluctuations in the system (*e.g.*, fluctuations of power demand or generation in renewable energy sources) is Markovian (in the above example the values of the demand at different times are independent) — it is then the function of both the system's state and a state of the Markov random process.

VI. NUMERICAL SOLUTION FROM BVP

There are two major ways to solve optimal control problems — [historically earlier] indirect [14] and direct [15] methods. Here we show how to obtain the MPFS trajectory by indirect method, *i.e.*, by solving the BVP (4b–7b). There are some similarities with multiple shooting and Gauss–Seidel methods.

If one tries to solve the BVP for the whole trajectory by quasi-linearization method or [multiple-]shooting with Newton's method, then the initial guess should be too close the the solution, otherwise Newton's iterations do not converge. Continuation method, with slow dragging of the final point to

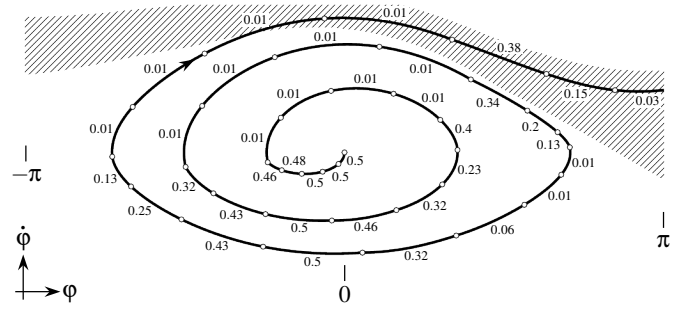


Fig. 10. Seed trajectory made of segments with duration 1. The value of the power demand P on each segment is written next to it.

$\varphi = \pi$, helps very little — the drag should be quite slow. The possible reason is that the whole MPFS trajectory has rich enough history with many features.

A way to overcome these difficulties is to solve BVP for small parts of the trajectory, such BVPs should be much simpler to deal with. The end points of the trajectory segment should be such that it is possible to go from $\mathbf{x}_{\text{start}}$ to \mathbf{x}_{end} in a straightforward manner for some realization of $\mathbf{u}(t)$. This is achieved by generating a suitable (*i.e.*, leading to failure) seed trajectory with a certain $\mathbf{u}(t)$, which is then gradually improved by optimizing its [not large] segments.

We generate the seed trajectory starting from NOP $\varphi = \dot{\varphi} = 0$ and adding to it one by one segments with constant value of P and with duration 1. If one chooses the new segment's value of P such that the value of φ_{end} at the right end of the segment is maximal, then one gets the solid curve trajectory from Fig. 3. The choice of the value of P such that the change of φ over the segment, $|\varphi_{\text{end}} - \varphi_{\text{start}}|$, is maximal gives the seed trajectory⁷ shown in Fig. 10. Initially we set $\boldsymbol{\beta}(t) \equiv 0$.

At the very start of the trajectory we have $\varphi = \omega = 0$. In the system of eqs. (4b–7b) no matter what is the starting value of $\boldsymbol{\beta}$, we have $P = P_*$ and don't leave NOP. We “jump-start” the trajectory by adding to it the solution of the BVP eqs. (4a,5a,7), that is better defined near NOP. Its duration should be large enough (we used 50). The boundary conditions are that we start at NOP and end up at some point of the seed trajectory that is close to NOP (we chose a point with 0.2 distance from NOP) — the power demand P is then far from $C^2/2$, and the eq. (6) is kept true.

In accordance with Bellman's principle of optimality [16] at the end of the trajectory we should have $P = P_*$ — if $\dot{\varphi} > 0$ we'll reach $\varphi = \pi$ anyway. We “relax” the trajectory by checking from where we can set $P = P_*$ and still get a failure.

Next we repeatedly choose a segment within the trajectory and attempt to optimize it. The segment's BVP, eqs. (4b–7b), is solved by simple shooting with Newton's method. The boundary conditions fix φ_{start} , ω_{start} , φ_{end} , and ω_{end} — they are not changed. The shooting parameters are $\boldsymbol{\beta}_{\text{start}}$ and the new duration of the segment. It is not crucial that the segment's BVP is solved right at the moment, so the maximal number of iterations N_{iter} in Newton's method is not needed to be large

⁷In general situation the creation of seed trajectory could be tricky, and additions of several new segments at once (checking all possible combinations of segments' control values) could be needed.

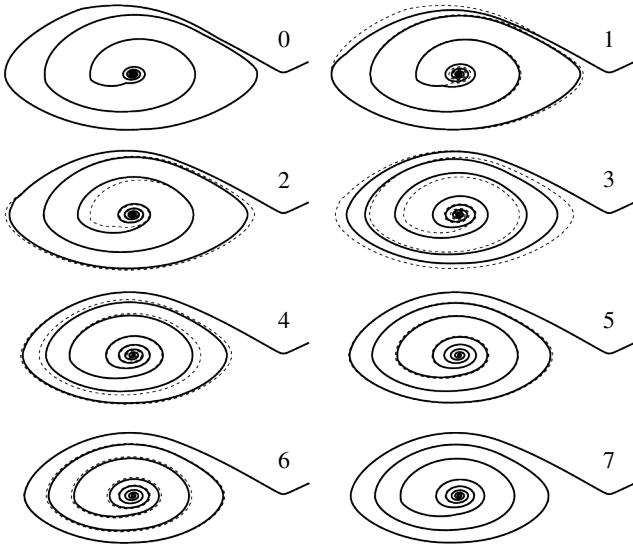


Fig. 11. The progress in obtaining the BVP solution. Attached to each trajectory is the number of completed passes. In upper left is the “jump-started” and “relaxed” seed trajectory from Fig. 10. The dashed thin curve provides the comparison with the trajectory from the previous pass.

(we used $N_{\text{iter}} = 10$). If the solution of the BVP is found, then it substitutes the old state of the segment. As the number of grid points could easily change, a doubly-linked list as a data structure for the trajectory is convenient.

The shorter is the segment, the smaller is its change due to optimization. If we work only with short segments, then the progress will be very slow. Thus, if obtaining the solution for the segment’s BVP was successful, we try the segment with the same starting point (with already updated value of β_{start}) but longer (we multiplied the duration of the segment by 1.25). Sometimes even if solving the BVP for a very short segment fails, it is beneficial to try a long segment anyway — it could throw a bridge over difficult trajectory parts (like the first 5 segments of the seed trajectory on Fig. 10, where $P \geq C^2/2$ results in the extreme values of $P_{\text{mech}} - \mathcal{P}(P, \varphi)$ which demands values of β to be large⁸).

If we fail to obtain the solution, then we shift the segment’s starting point forward by a share of its length (we shifted to a random point in the first half of the segment) and try again. The value of β could be already non-zero [and close to being reasonable] from previous successes. Eventually we complete a “pass” — go through the whole trajectory. We continue to run passes until the trajectory converges.

The gradual convergence of the trajectory to the optimal solution is shown in Fig. 11.

VII. PROBABILITY OF FAILURE

When both φ and ω are small, and $P \approx P_*$, we can write the linearized equations of motion near NOP as

$$\ddot{\varphi} + D\dot{\varphi} = -(P - P_*)/2 - 7\varphi/16. \quad (8)$$

When the average number of consuming customers is large, $\lambda \gg 1$, and the width of the time chunk is small, $\delta \ll 1$, we can

think about $P - P_*$ as a noise with small correlation time. It has (as $\mathbb{E}P(t) = P_*$, $\mathbb{E}P^2(t) = P_*^2(1 + 1/\lambda)$) zero mean and the integral of its autocovariance function over time is equal to $P_*^2\delta/\lambda$. This results in probability distribution of the system’s state being mainly a Gaussian distribution with NOP $\varphi = \dot{\varphi} = 0$ as its center. After some calculations we get the probability density function $f(\varphi, \dot{\varphi}) \propto \exp(-(\lambda/\delta)4D(7\varphi^2 + 16\dot{\varphi}^2))$. This can be obtained, *e.g.*, by directly treating the stochastic system (8) or by solving the linearized MPFS equations (4c) with $\rho = -16D$ and the boundary condition that the trajectory ends at the state $(\varphi, \dot{\varphi})$.

This found Gaussian center of the probability distribution could be used for a naive estimate of the probability of failure. We are interested in reaching $\varphi = \pm\pi$, so the probability of failure in unit time is $\text{P}(\text{failure}) \sim f(\pi, 0) \sim \exp(-(\lambda/\delta)28D\pi^2)$.

From (3) we estimate $\text{P}(\text{failure}) \sim \exp(-(\lambda/\delta)\mathcal{S})$. Of course, $\exp(-(\lambda/\delta)\mathcal{S})$ is not the realization probability of the most probable trajectory that leads to a failure. The expression (3) contains also the factor $1/\sqrt{2\pi n}$ for each chunk of time, which makes the probability of that very trajectory to be much smaller than $\exp(-(\lambda/\delta)\mathcal{S})$. But the most probable trajectory is not the only trajectory that leads to a failure. Lots of trajectories that are close to the MPFS trajectory also cause a failure. To accurately find the failure probability, we need to take into account all such trajectories.

Exploring the vicinity of the MPFS trajectory is similar to the study of the saddle point in the method of steepest descent. This is typically a very hard task. Luckily, we often may skip it. The MPFS trajectory (position of the saddle point) provides the exponential part of the answer $\exp(-(\lambda/\delta)\mathcal{S})$, while taking into account the whole bunch of trajectories (integrating in the vicinity of the saddle point) provides the pre-exponential correction which is less important.

Considering the MPFS trajectory over infinite interval of time $(-\infty, 0)$, we get infinitely many time chunks, and thus $1/\sqrt{2\pi n}$ factors. At the same time the integral $\mathcal{S} = \int_{-\infty}^0 dt H(P(t)/P_*)$ converges because the integrand exponentially decays when t tends to $-\infty$. The probability of the MPFS trajectory realization, strictly speaking, is equal to 0. The probability of failure is not, because in this case there are infinitely many different trajectories that end up in failure. As $D > 0$, the details of the system evolution in a very distant past are not important — they are forgotten because of the decay. The value of n_k of the k^{th} chunk of time in the distant past doesn’t affect whether the failure did happen or not, and taking into account all trajectories that end up in failure means summation over n_k which eliminates the factor $1/\sqrt{2\pi n_k}$.

The whole part of the MPFS trajectory (which can be seen in Figs. 6 and 7) that is inside the [Gaussian] center of the probability distribution is irrelevant — the variation of the trajectory there hardly affects the outcome of the evolution. The larger is λ/δ , the smaller is this part (and the smaller is the probability $\text{P}(\text{failure})$). The meaningful part of the MPFS trajectory is the one outside of the region where the system spends most of its time.

Although the probability distribution of the system’s state has its center being close to Gaussian, its tails are not contin-

⁸Such artifacts in seed trajectory should be avoided if possible.

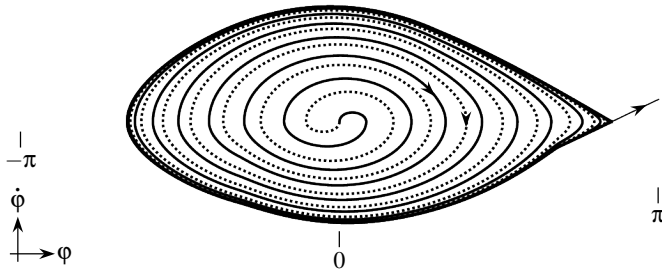


Fig. 12. Two trajectories of the system (2) with P at each moment of time being chosen (with a condition $|P - P_*| < P_{\text{control}}$) in order to have maximal if $\dot{\phi} > 0$ and minimal if $\dot{\phi} < 0$ possible value of thrust $P_{\text{mech}} - \mathcal{P}(P, \phi)$. Thick solid/dotted curve corresponds to starting condition being NOP $\phi = 0$, $\dot{\phi} = 0$, with the initial thrust in positive/negative direction. The used value of $P_{\text{control}} \approx 0.1385$ is the minimal one for which it is possible to bring the system to $\phi = \pi$ state.

uing the trend. To see how strongly the naive estimation from the Gaussian center is wrong, we can compare for $D = 0.1$ the numerical values of $\mathcal{S} \approx 4.6806$ and of $28D\pi^2 \approx 27.6$. Their ratio is about 5.9, and these numbers are in the exponent. With such a difference, if for example we naively estimate the probability of failure in unit time as about 10^{-12} , then the actual probability could be not far from 10^{-2} . This illustrates the danger of estimating the probability of rare events from such characteristics of the probability distribution as mean value and standard deviation.⁹ Same sentiments against widespread assumption of Gaussian or normal statistics were expressed, *e.g.*, in [17].

There could be situations where instead of failure probability the relevant question is whether a malicious party that controls part of a grid could bring the system to failure. For an example, see Fig. 12.

VIII. CONCLUSIONS

Even if a power system is “statically stable”, *i.e.*, no constant in time choice of such parameters as power demands at loads or production by generators could drive the system to a non-operating state, by varying these parameters in time we may be able to bring the system to a failure.

While designing a power system, it is interesting to know what is the probability per unit time that causing a failure fluctuation would occur. This probability can be effectively estimated by optimal fluctuation method [4], in which the most probable evolution leading to a failure is a solution to a certain optimal control problem.

The equations for the “optimal” failure trajectory are sensitive to the details of random power demand or generation statistics. For accurate estimates of a failure probability, realistic models of various power grid components with randomly varying parameters need to be developed.

REFERENCES

- [1] I. Dobson and H.-D. Chiang, “Towards a theory of voltage collapse in electric power systems,” *Syst. Control Lett.*, vol. 13, no. 3, pp. 253–262, 1989.

⁹One need not think that assumption of Gaussian statistics always underestimates the probability of a rare event. Consider, *e.g.*, our model power grid with D being large enough, so it is impossible to bring the system to $\phi = \pm\pi$.

- [2] I. Dobson, B. A. Carreras, V. E. Lynch, and D. E. Newman, “Complex systems analysis of series of blackouts: Cascading failure, critical points, and self-organization,” *Chaos*, vol. 17, no. 2, p. 026103, 2007.
- [3] J. Salmeron, K. Wood, and R. Baldick, “Worst-case interdiction analysis of large-scale electric power grids,” *IEEE Trans. Power Syst.*, vol. 24, no. 1, pp. 96–104, 2009.
- [4] I. M. Lifshitz, “The energy spectrum of disordered systems,” *Adv. Phys.*, vol. 13, no. 52, pp. 483–536, 1964.
- [5] B. I. Halperin and M. Lax, “Impurity-band tails in the high-density limit. I. minimum counting methods,” *Phys. Rev.*, vol. 148, no. 2, pp. 722–740, 1966.
- [6] J. Zittartz and J. S. Langer, “Theory of bound states in a random potential,” *Phys. Rev.*, vol. 148, no. 2, pp. 741–747, 1966.
- [7] A. A. Belavin, A. M. Polyakov, A. S. Schwartz, and Y. S. Tyupkin, “Pseudoparticle solutions of the Yang–Mills equations,” *Phys. Lett. B*, vol. 59, no. 1, pp. 85–87, 1975.
- [8] L. N. Lipatov, “Divergence of the perturbation-theory series and the quasi-classical theory,” *Sov. Phys. JETP*, vol. 45, no. 2, pp. 216–223, 1977.
- [9] G. Falkovich, I. Kolokolov, V. Lebedev, and A. Migdal, “Instantons and intermittency,” *Phys. Rev. E*, vol. 54, no. 5, pp. 4896–4907, 1996.
- [10] M. Chertkov, F. Pan, and M. G. Stepanov, “Predicting failures in power grids: the case of static overloads,” *IEEE Trans. Smart Grids*, vol. 2, no. 1, pp. 162–172, 2011.
- [11] M. Chertkov, M. Stepanov, F. Pan, and R. Baldick, “Exact and efficient algorithm to discover extreme stochastic events in wind generation over transmission power grids,” in *2011 50th IEEE Conference on Decision and Control and European Control Conference (CDC-ECC)*, 2011, pp. 2174–2180.
- [12] W. W. Price, H.-D. Chiang, H. K. Clark, C. Concordia, D. C. Lee, J. C. Hsu, S. Ihara, C. A. King, C. J. Lin, Y. Mansour, K. Srinivasan, C. W. Taylor, and E. Vaahedi, “Load representation for dynamic performance analysis,” *IEEE Trans. Power Syst.*, vol. 8, no. 2, pp. 472–482, 1993.
- [13] P. C. Martin, E. D. Siggia, and H. A. Rose, “Statistical dynamics of classical systems,” *Phys. Rev. A*, vol. 8, no. 1, pp. 423–437, 1973.
- [14] L. S. Pontryagin, V. G. Boltyanskii, R. V. Gamkrelidze, and E. F. Mishchenko, *The mathematical theory of optimal processes*. New York: Interscience Publishers, 1962.
- [15] J. T. Betts, *Practical methods for optimal control using nonlinear programming*. Philadelphia: SIAM, 2001.
- [16] R. Bellman, *Dynamic programming*. Princeton: Princeton University Press, 1957.
- [17] G. Falkovich, I. Kolokolov, V. Lebedev, V. Mezentsev, and S. Turitsyn, “Non-Gaussian error probability in optical soliton transmission,” *Physica D*, vol. 195, no. 1–2, pp. 1–28, 2004.